applied sciences

MDPI

Article

Development of a Process Simulation Model for the Analysis of the Loading and Unloading System of a CNG Carrier Equipped with Novel Lightweight Pressure Cylinders

Rodolfo Taccani [1,*], Gabriele Maggiore [2] and Diego Micheli [1]

[1] Department of Engineering and Architecture, University of Trieste, 34127 Trieste, Italy; micheli@units.it
[2] Cenergy srl, c/o Area Science Park, Basovizza, 34149 Trieste, Italy; gabriele.maggiore.94@gmail.com
* Correspondence: taccani@units.it

Received: 31 August 2020; Accepted: 23 October 2020; Published: 27 October 2020

Abstract: Natural gas is becoming increasingly important to meet the growing demand for energy, guaranteeing a reduction in polluting emissions. Transportation in form of Compressed Natural Gas (CNG) could be an alternative to the traditional transportation by pipeline or, as liquefied gas, by ships, but the ratio between the mass of transported gas and the container weight is currently too low. One of the many projects focusing on the development of innovative lightweight pressure cylinders is GASVESSEL, which proposes composite cylinders with a diameter of more than 3 m: loaded on a ship, they could allow transporting quantities of CNG as big as 10,000 tons. The related loading and unloading processes affect both the overall time required for transport and the quantity of transported gas; therefore, they have an impact on the economic feasibility of the whole project. In this paper, a newly developed process simulation model is presented that allows assessing the duration of the loading and unloading processes, the mass of transported CNG, and the amount of power and energy required by the process. The model is useful to support the design of the system considering different plant components and operating strategies. It is applied to the analysis of the loading and unloading of a ship that meets the GASVESSEL project specifications. The results show that the duration of the process is of the order of magnitude of 100 h, depending on ambient temperature, and that the energy consumption can vary in the range of 150–180 kJ for a unit mass of CNG. Finally, the model is used to simulate the same process with hydrogen, an energy carrier that allows meeting, together with the use of fuel cells, the requirements of zero local emissions. The results show increments of both the final loading temperature and compressor power with respect to the CNG case.

Keywords: CNG transportation; CNG carrier; CNG loading model

1. Introduction

Natural Gas (NG) has a central role, in the global energy scene, in the shift to an economy with lower pollutant emissions. It is currently in second place, behind oil and together with coal, when it comes to global energy consumption, with a percentage close to 24% [1]. Globally, it has seen from 2010 the second highest demand growth rate, after renewable sources. According to [1], in 2040, NG should exceed coal by about six percentage points, in order to satisfy global energy needs.

The traditional systems for the supplying of NG are mainly two: the transportation of Liquefied Natural Gas (LNG) by ships and the conveyance into pipelines. An alternative system is the transportation using pressure cylinders. This method is often referred to as Compressed Natural Gas (CNG). The advantages of CNG, with respect, in particular, to LNG, can be summarized as follows:

- The exploitation of stranded gas fields or flare and associated gas can be economically viable [2,3];
- It is an economic way of transporting small quantities of gas and exploiting small reserves [3];
- It can be an economic way of transporting ng over short distances, between 800 and 3000 km, or 250–5000 km, making also use of cooling [2];
- The containment of costs due to the lack of liquefaction and regasification plants;
- The return time of the investment can be shorter;
- The largest investment (85%) for cng concerns the ship, which is a mobile value that can be used in other places, while for an lng project, 60% of the cost falls within liquefaction and regasification plants [4], which cannot be used in other places;
- CNG does not have the problem of the loss of load due to the boil off.

CNG technology consists of compressing the gas at high pressure, from 200 up to 300 bar. The volume reduction is 200–300 times compared to those in standard conditions [2,3]. However, the density of CNG is at most equal to about half of that of the LNG (218 kg/m^3 for methane at 300 bar and 20 °C versus 415 kg/m^3 for LNG at 1 bar and 162 °C), but the energy consumption of the compression process is about half of that required by liquefaction and regasification. Once compressed, the gas is stored in tanks placed on the ship and transported near a gas pipeline, where it is discharged at high pressure.

Therefore, the most important phases of this transport technology are the following:

- Gas treatment;
- Compression and possible cooling;
- Loading and transport with ships;
- Reception and unloading by decompression.

The safety of this technology can be a problem, but since the discharge can take place offshore, some kilometers away from the coast, the risks remain confined and do not concern entire populated areas, as is the case for the LNG technology regasification terminals. In any case, the risk related to the storage of a flammable substance at high pressure was one of the problems that in the past did not allow an important development of this technique. Technological development with regard to storage tanks has allowed this transport system to become more efficient and safer. In particular, the introduction of composite materials has brought greater safety and, at the same time, a considerable weight saving [2].

The first CNG transport project using ships dates back to the 1960s and involved the use of a series of vertical cylinders [2]. This project was abandoned due to the very high cost of pressure vessels. Subsequently, the renewed interest in the technology has led to the development of some alternatives. In the last decade of the last century, Cran and Stenning designed a new type of pressure tank called Coselle [2,3] (from the English “coil”, winding, and “carousel”, bobbin). Later, new technologies emerged such as the Volume Optimized TRANsport and Storage (VOTRANS) [2,3] of EnerSea Transport, the Pressurized Natural Gas (PNG) [2] of Knutsen OAS, the Gas Transportation Module (GTM) [2,3] of TransCanada, the Composite Reinforced Pressure Vessel (CRPV) [2] of Trans Ocean Gas (TOG), and the Compressed Energy Technology (CETech) [3]. Tables 1a and 1b, adapted from [3], with the only addition in the last column of Table 1b of the GASVESSEL project [4], shows a summary of the various technologies. As far as the ratio between the gas transported and the weight of the containers is concerned, only the weight of the tanks without valves, pipes, and flanges is considered.

The first and only CNG ship currently in service, the “Jayanti Baruna”, was launched in January 2016 in Indonesia and has a capacity of 0.67 MNm^3 @250 bar of gas, allowing linking East Java with the island of Lombok. The gas is stored in an 832 vertical cylinder (height 12 m, diameter 615 mm, thickness 19 mm), and the ratio container/cargo weight is 0.15 [4].

Therefore, the currently too low ratio between the mass of transported gas and the vessels–cargo weight can be considered one of the reasons why CNG technology currently has such a limited diffusion.

Table 1. CNG vessel technologies, part a,b.

(**a**)				
	GEV Coselle	**GEV Optimum**	**VOTRANS**	**Knutsen PNG**
containment	coiled X-80 steel pipe forming a carousel	API 5LX80 steel pipes	X-80 steel cylinders	X-80 steel cargo tank cylinders
arrangement	coiled pipe in holds	horizontal in holds	vertical tanks modules or horizontal pipes	vertically stacked
gas press. (bar)	200–275	250	125	250
gas temp. (°C)	ambient	ambient	−30	ambient
cargo/container weight ratio	0.12–0.18	0.4	0.35–0.39	0.21
development stage	advanced concept	advanced for 5.5 MNm3	advanced	concept
capacity (MNm3)	1.5–15	5.5–12.5	2–30	2–35
(**b**)				
	TOG	**TransCanada**	**CeTech**	**GASVESSEL**
containment	composite HDPE and fiberglass cylinders (MEGC)	composite reinforced steel GTMs	composite or X-80 steel pipes	composite reinforced steel
arrangement	container or modular cassettes with vertical cylinders	GTMs stacked (cylinders)	vertical/horizontal	vertical
gas press. (bar)	250	206	150–250	300
gas temp. (°C)	ambient/−30	ambient	ambient/−30	ambient
cargo/container weight ratio	0.34/0.47	1.5	0.7 (composite) 0.24 (X-80 steel)	1.5
development stage	concept	concept	concept	advanced concept
capacity (MNm^3)	7	0.3–3	7–15 (composite) 8–35 (steel)	12

However, the problems relating to loading and unloading processes must also be considered. These processes affect both the overall time required for transport and the quantity of transported gas and, therefore, they have an impact on the economic feasibility of the whole project.

Based on these considerations, in this paper, it is first shortly described the GASVESSEL project, which focuses on the development of innovative lightweight composite pressure cylinders with a diameter of more than 3 m: loaded on a ship, they could allow transporting quantities of CNG as big as 10,000 tons [4]. Then, a newly developed process simulation model is presented and realized in the Matlab® environment, which allows assessing the duration of the loading and unloading processes, the mass of transported CNG, and the amount of power and energy required by the process. The model is useful to support the design of the system considering different plant components and operating strategies.

Almost all the calculation models of the filling and emptying processes of CNG tanks found in the literature refer to the use of CNG to power road vehicles with spark ignition engines, replacing petrol. In fact, today, this is the most widespread use of CNG (the share is about 1.6% in total vehicle feet worldwide [5]), while the use as a supplying system of NG on ships is currently under development. The gas is taken from the low-pressure distribution network, and then, it is compressed in the storage tanks of the filling station. Then, the vehicle's cylinder is filled by the pressure difference.

These models are based on the first law of thermodynamics, appropriate assumptions about components efficiency, and on the choice of a suitable Equation of State (EOS) for the calculation of the thermodynamic properties of NG, which are treated as a real gas. The main problems are related to the so-called Fast Filling Process (FFP). They concern the reduction of the filling time without an excessive reduction of the fill efficiency. The fill efficiency is the ratio of the actual filled mass to the capacity at the rated pressure and ambient temperature. The underfilling is due to the heat generated by the re-compression of CNG in the cylinder. Another problem is the required compressor input work,

which is then partially wasted during FFP. In turn, the filling time, underfilling, and compression work also depend on the gas composition, ambient temperature, storage type, and compressor performance.

The first FFP model was presented by Kountz. In [6], with reference to a CNG storage cylinder, he found a rise of 40 °C of the storage gas temperature. It is also shown by Kountz that the fast fill of CNG cylinders, at 20 °C ambient temperature, typically achieves a fill efficiency of 80%. In [7], two methods are compared for storing fuel in CNG stations, namely buffer storage and three pressure levels cascade storage systems. The authors found that the filling time is lower and the charged mass is higher with buffer storage, whilst the compressor work is lower with cascade storage. In [8], the authors studied an FFP based on a three-stage compressor and both buffer and cascade configurations, which are referred to as a single storage system (SSS) and cascade storage system (CSS). The optimum amounts of inter-stage pressure have been found for every configuration using the particle swarm optimization (PSO) algorithm. They too found that SSS allows a low refueling time and high filling ratio, while CSS allows reducing the energy consumption.

The influence of NG composition is investigated in [9] using the AGA8 EOS to calculate the thermodynamic properties of NG with methane percentage in the field 87–98.6%. They found that the composition has a small effect on the filling time but significant effects on the charged mass, with variations around 20%. In another work [10], the same authors, using a detailed model of a reciprocating compressor with automatic valves, found that natural gas composition, with methane percentage varying from 79% to 98%, has significant effects on compressor performance. The consuming work per cycle and the mean discharge temperature increases with methane percentage.

In [11], the authors investigate the FFP of NG in Type-III cylinders, which have a metal liner and a full-wrapped composite reinforcement, for heavy-duty vehicles with and without active heat removal in order to improve the fill efficiency. The active heat removal system involves placing cooling coils inside the cylinder through which a coolant is circulated. The passive heat removal system involves pre-chilling thermal heat sinks in the cylinder. In [5], the results are presented of the operational and safety tests of a CNG home fast refueling station based on a one-stage hydraulic compressor.

A problem somewhat closer to that covered by the present paper is addressed in [12]. A mathematical model is developed to simulate the filling process of high-pressure tankers for marginal gas wells. Then, the model is validated against experimental data obtained from a marginal gas well.

In this paper, the newly developed model is applied to the analysis of the loading and unloading of a ship that meets the GASVESSEL project specifications.

Finally, the model is used to simulate the same process with hydrogen, which is an energy carrier that allows meeting, together with the use of fuel cells, the requirements of zero local emissions.

2. The GASVESSEL Project

The four-year project GASVESSEL [4], funded by the EU H2020 research and innovation programme, started in June 2017 and was proposed by a consortium formed by thirteen partner companies from eight countries (Belgium, Cyprus, Germany, Greece, Italy, Norway, Slovenia, and Ukraine). The main design data of the pressure vessel and of the ship considered in the project are reported in Table 2.

The pressure vessels arrangement in the CNG carrier ship is vertical. To reduce fire hazard, the holds are saturated with nitrogen. The pressure vessels are made of austenitic stainless steel liner (5 mm) externally reinforced with a composite made of carbon fiber and impregnated with epoxy resin (35 mm).

Table 2. GASVESSEL project [4]: CNG vessel and ship design main specifications.

Pressure Vessel Main Specifications:	
gas cylinder outer diameter	3.4 m
gas cylinder length	22.5 m
volume (water)	175 m^3
vessel mass capacity, referred to CH_4 @300 bar, 20 °C	38 ton
design pressure	300 bar
CNG ship design:	
length, overall	205 m
max breadth	36 m
height to main deck	22.0 m
design draft	7.5 m
n° vessels in the CNG ship	272
total vessels volume (water)	44800 m^3
total gas mass @ 300 bar 20 °C (*)	9771 ton
total gas volume	13.762 MNm^3
cargo gas/container weight ratio	1.5

* referred to pure methane.

3. Plant Arrangements and the Loading and Unloading Processes

The schematics of the kind of CNG plant considered in this study are shown in Figure 1, in both the loading (a), and unloading (b), configurations. The compressor, with its control valves and CNG cooler, is installed on board the ship. The two valves mounted before and after the compressor introduce a variable pressure drop, allowing the machine to operate in non-flooding conditions. The cooler always presents after the compressor to maximize the compressed gas density. During the loading phase, the suction is connected to the storage terminal and delivers to the pressure vessels. During the unloading phase, the suction is connected to the pressure vessels, with the interposition of a heater, while the delivery is connected to the pipeline. The heater is used only in the unloading configuration, because the temperature of the pressure vessels can reach process values as low as −60 °C, due to the expansion of the gas contained in it. In both configurations, a by-pass allows the compressor to be excluded from the circuit when the flow occurs spontaneously due to the pressure difference.

In fact, the loading and unloading processes are divided into two subsequent free and forced phases. During the free phases, the gas flow is due to the pressure difference between the pressure vessels and the storage terminal or the pipeline, respectively. During the forced phases, the compressor provides the pressure vessels with complete filling in the loading process and the most complete as possible emptying in the unloading one. By acting on the lamination valve placed on the intake, the compressor can operate even when the pressure of the upstream tanks is higher than that of the downstream pipeline. For example, this is necessary when the flow in the free discharge phase falls below 20 kg/s; therefore, it is more convenient to operate the compressors to speed up the process.

Since the required volume flow rates and compression ratios are not excessively low or high, they can be obtained with both centrifugal and volumetric compressors.

In a centrifugal compressor, the maximum flow is limited by choking, the minimum flow is limited by surge, and the compression ratio is a function, other than of stages number and geometry, of gas molecular weight and compressibility. In a volumetric compressor with automatic valves, the flow rate is proportional to the speed of rotation, while the stage compression ratio is independent from it and less sensitive, with respect to the centrifugal ones, to changes of the composition of the fluid. On the other hand, the composition of NG depends on the field of origin, but the variation of the mean molecular weight, density, and other physical properties is not so large as to prefer the use of volumetric compressors for this reason.

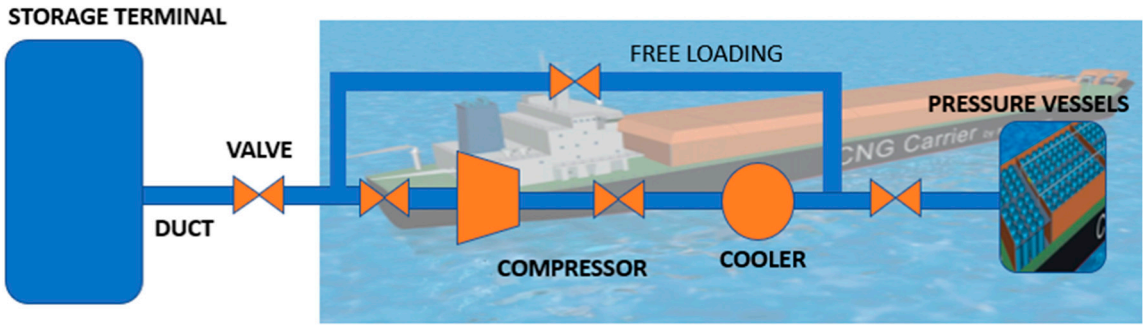

(**a**) loading plant

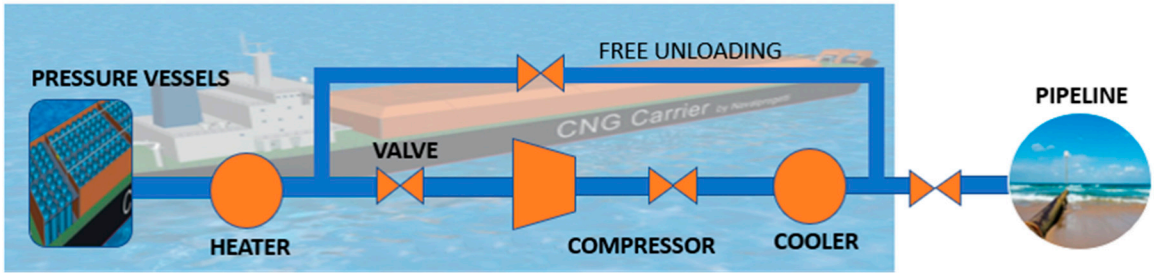

(**b**) unloading plant

Figure 1. Schematic of the loading (**a**), and unloading (**b**), CNG plants.

Reciprocating compressors have very high adiabatic efficiency, but as compression ratio drops, adiabatic efficiency drops. However, with NG, the drop is limited, and adiabatic efficiency can be 93% at a compression ratio of 3 and 91% at a compression ratio of 1.4 [13]. In centrifugal compressors, the polytropic efficiencies range from 70% to 85%, and efficiencies approaching 90% are possible. The corresponding values of adiabatic efficiency depend on the compression ratio, but they will be in general lower than those of reciprocating compressors.

In terms of costs, generally, a reciprocating compressor will have a lower CAPital EXpenditure (CAPEX), since centrifugal ones use complex geometry parts, but they will have a higher Operating EXpenditure (OPEX), because a centrifugal compressor has fewer wearing parts, resulting in lower operating costs in terms of replacement parts, repairs, and downtime (high reliability). Moreover, with centrifugal compressors, there are no vibrations.

In conclusion, at the end of this analysis, it was decided to evaluate the adoption of centrifugal compressors, considering the lower operating costs and the higher reliability as main arguments.

4. Model Equations

The equations of the model describe the behaviors of all the components of the systems reported in Figure 1, i.e.,

- Vertical cylindrical tanks;
- Regulation valves; Cooler/heater;
- Centrifugal compressors;
- Ducts.

NG cannot be treated as an ideal gas under the thermodynamic conditions considered here. Various approaches are described in the literature for the calculation of its properties as real gas, with particular reference to the filling of small tanks for automotive applications [8,13]. In this work, the gas properties in all the components of the loading and unloading plant are obtained from the National Institute of Standards and Technolgy (NIST) database by using the open source software tool Coolprop, which allows considering both pure components, as CH_4, and various NG mixtures,

as those found in [14]. For CH_4 calculations, the considered EOS is described in [15], while in the case of mixtures, the calculations employ a model that applies mixing rules to the Helmholtz energy of the components. The departure function from ideal mixing is consistent with the GERG model [16].

4.1. The Tank Model

The time-dependent variables of the tank model are (see Figure 2, where the tank is referred to as a Receiver Vessel):

- Gas pressure, p_r;
- Gas temperature, T_r;
- Mass of gas, m_r;
- Cylinder wall temperature, T_w.

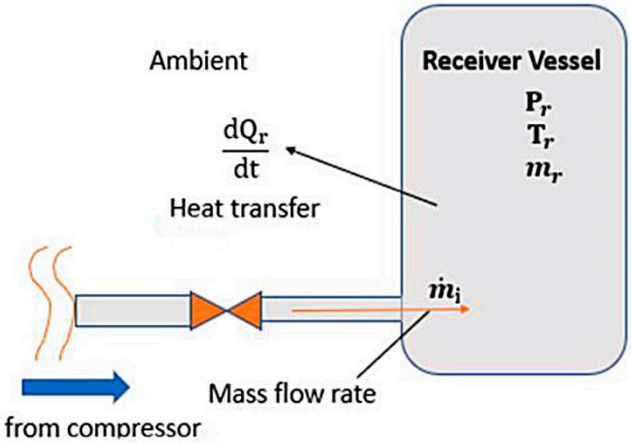

Figure 2. Scheme representing the variables of the receiving tank.

Some hypotheses have been made to simplify the equations characterizing this element:

- The potential energy linked to any difference in altitude between the storage terminal and the tank is neglected;
- The kinetic energy of the gas inside the tank is neglected;
- The pressure and temperature of the gas inside the tank does not depend on the spatial coordinates (perfect mixing hypothesis);
- The mass flow rate is calculated, in the case of free loading/unloading, as an isenthalpic expansion through an orifice while, if the compressors is used, it is taken from the machine characteristic curve, once the compression ratio is known;
- The heat exchange from the control volume of the tank to the wall is described by a convective heat flow toward the wall, which is considered a concentrated mass: this implies that the cylinder wall temperature does not depend on the spatial coordinates but assumes a uniform average value.

The equations needed to calculate the values of the tank model variables are:

- Conservation of mass:

$$\frac{dm_r}{dt} = \dot{m}_i \tag{1}$$

- Energy balance:

$$\frac{d(m_r \cdot u_r)}{dt} = \dot{m}_i \left(h_i + \frac{v_i^2}{2} \right)_i + \frac{dQ_r}{dt} \tag{2}$$

- Mass flow rate:

  (a) Free loading cases:

$$\dot{m}_i = C_d \cdot A \cdot \sqrt{2p_i \cdot \rho_i \frac{k}{k-1}\left[\left(\frac{p_r}{p_i}\right)^{\frac{2}{k}} - \left(\frac{p_r}{p_i}\right)^{\frac{k+1}{k}}\right]} \quad \text{if} \quad \frac{p_r}{p_i} > \left(\frac{2}{k+1}\right)^{\frac{k}{k-1}} \tag{3}$$

$$\dot{m}_i = C_d \cdot A \cdot \sqrt{k \cdot p_i \cdot \rho_i \left[\left(\frac{2}{k+1}\right)^{\frac{k+1}{k-1}}\right]} \quad \text{if} \quad \frac{p_r}{p_i} \leq \left(\frac{2}{k+1}\right)^{\frac{k}{k-1}} \tag{4}$$

  (b) Forced loading cases: centrifugal compressor curves (see Section 4.4)

- Cylinder wall temperature:

$$\frac{dT_w}{dt} = \frac{1}{m_w C p_w}\left(-\frac{dQ_r}{dt} - \frac{dQ_{amb}}{dt}\right) \tag{5}$$

where assuming that natural convection is dominant, the internal heat flux of the vessel is:

$$\frac{dQ_r}{dt} = -\alpha_i S_i \left(T_r - T_w\right) \tag{6}$$

and the external heat flux between the vessel surface and the atmosphere is:

$$\frac{dQ_{amb}}{dt} = \alpha_e S_e \left(T_w - T_{amb}\right). \tag{7}$$

The internal convective heat exchange coefficient, α_i, is obtained by the value calculated for the Nusselt number, while for the external one, it is assumed $\alpha_e = 4.5$ W/m^2/K [17].

The equations have been rearranged in order to calculate at each time step the mass of CNG and the temperature in the tank. Then, after the calculation of the gas density as the ratio between the mass and the tank internal volume, the pressure and all the other thermodynamic properties of interest are calculated by means of Coolprop.

4.2. The Regulation Valves Model

The type of formulation used to tie the pressure loss through the valve with the mass flow rate is the so-called universal gas sizing method [18,19]. Applying this method, the mass flow rate is given by Equation (8), where pressures must be introduced in *psia*.

$$\dot{m} = 1.06\, C_g \cdot \sqrt{p_i \cdot \rho_i} \cdot \sin\left(\frac{59.64}{C_1} \cdot \sqrt{1 - \frac{p_o}{p_i}}\right) \tag{8}$$

The valve manufacturers supply the gas flow-sizing coefficient, C_g, in conditions of maximum opening. The coefficient $C_1 = C_g/C_v$ can be assumed equal to 25 if the value of the fluid flow size coefficient C_v is unknown. The correlation between the coefficient and percentage of opening depends on the type of characteristic of the valve, which can be a linear, equal-percentage, or quick opening.

4.3. The Cooler/Heater Model

The heat power transferred in the heat exchangers is given by Equation (9):

$$Q_{hex} = \dot{m}(h_i - h_o). \tag{9}$$

The pressure drop is assumed to be one percentage point of the pressure at the heat exchanger inlet.

4.4. The Centrifugal Compressor Model

The centrifugal compressor is modeled by means of its characteristic curves. They are provided by the manufacturer and eventually manipulated to be represented in the form of compression ratio, β, as a function of the corrected mass flow rate, $\dot{m}\sqrt{T_{01}}/p_{01}$, for different values of the corrected rotational speed, $n/\sqrt{T_{01}}$, as shown in Figure 3. The corresponding values of the polytropic efficiency, η_p, are also provided by the manufacturer.

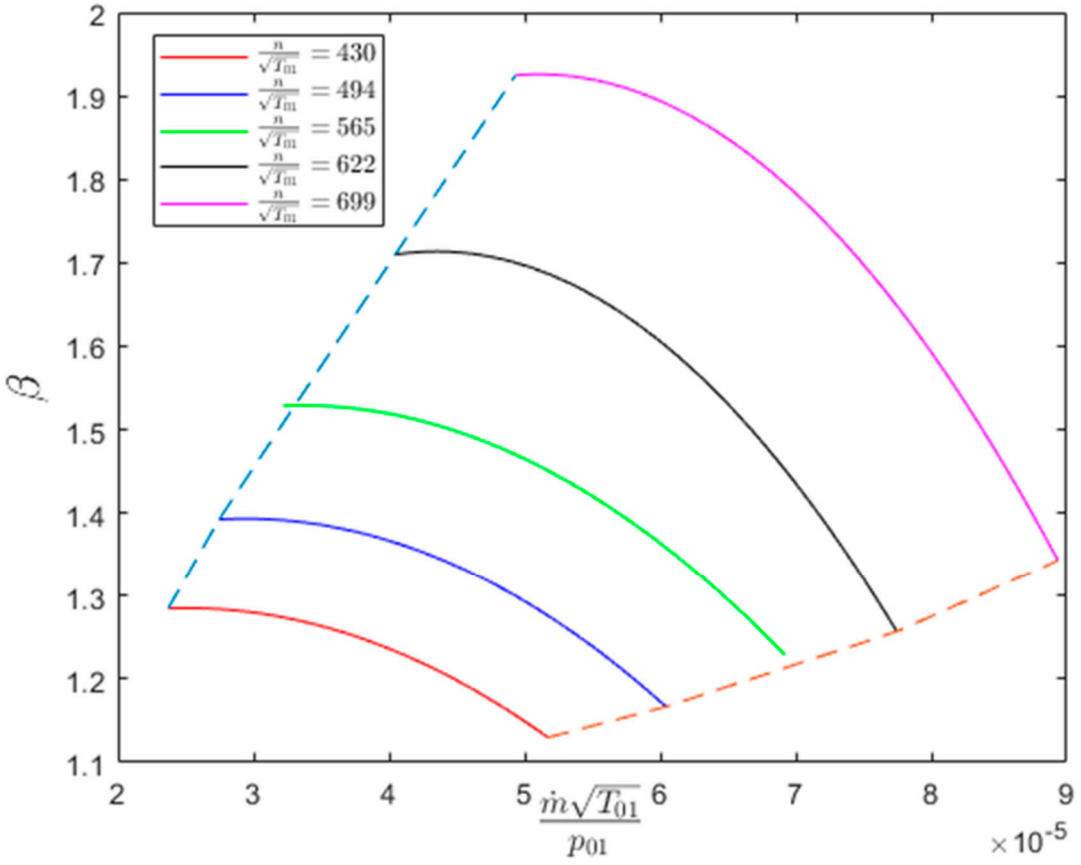

Figure 3. Compressor characteristic curves.

Then, the input parameters of the compressor model are the stagnation temperature and pressure at suction, T_{01} and p_{01}, respectively, and the compression ratio. The last one is determined by *(i)* the tank pressures, *(ii)* the pressure drop in the ducts, and *(iii)* the pressure losses introduced by the valves. Once the compression ratio is known, the mass flow rate and the polytropic efficiency can be obtained from the characteristic curves. Then, the absorbed power is given by Equation (10):

$$P = \dot{m} \cdot \frac{n}{n-1} Z R T_{01} \left(\beta^{\frac{n-1}{n}} - 1 \right) \cdot \frac{1}{\eta_p}. \tag{10}$$

The temperature of the gas leaving the compressor is calculated given the corresponding enthalpy and pressure values.

4.5. The Ducts Model

For the calculation of the two pipes present in the plant diagrams, one upstream and one downstream of the compressor, the following hypotheses have been introduced:

- One-dimensional flow;
- Perfect gases, with specific heat at constant pressure function of temperature only;

- Uniform gas properties in the duct.

With these hypotheses, the mass and momentum conservation equations for the duct are:

$$\frac{dp_i}{dt} = \frac{kRT_i}{AL}\left(\dot{m}_i - \dot{m}_o\right) \tag{11}$$

$$\frac{d\dot{m}_o}{dt} = \frac{A}{L}\left(p_i + p_o\right) - \frac{\lambda RT_i \dot{m}_o{}^2}{DA(p_i + p_o)} \tag{12}$$

where the Darcy friction factor λ is derived from the Moody diagram.

5. Model Validation

The validation of the model was carried out by comparison with experimental literature data. In [20], the authors consider the filling of the cylinder shown in Figure 4: it has an aluminum liner with a reinforcement in composite material (epoxy resin with carbon fiber). The diameter is 396 mm, the length 830 mm, and the internal volume 70 L. The service pressure is 207 bar, and it is fed by a supply unit of 450 L at a pressure of 400 bar.

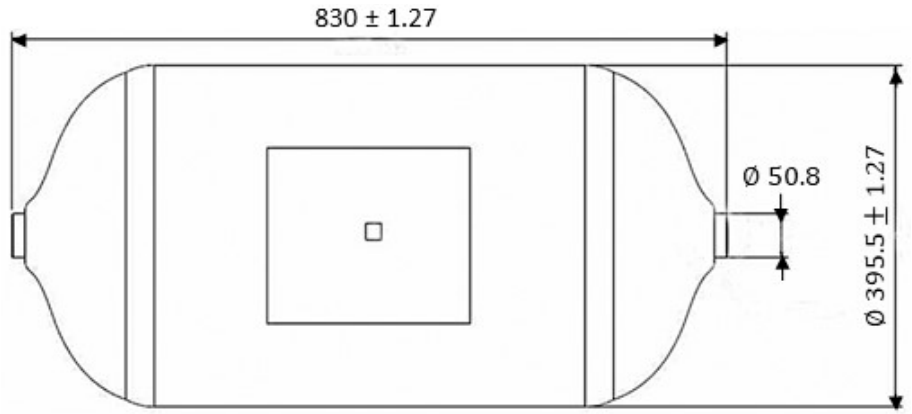

Figure 4. Geometry of the type III CNG cylinder considered for the model validation [20].

The average temperature reported in [20] has been compared with the simulation results. Temperature data are of particular interest, because the safety of the cylinders in the composite material is verified when going to study the temperature rise that occurs during the compression of the gas.

The ambient temperature is not given in the paper, and therefore, it was assumed to be 25 °C, since the measurements were performed in a summer period. The initial cylinder temperature is −8 °C, and its initial pressure is 10 bar. The results obtained are shown in Figure 5. The final temperature reached by the numerical model is 41 °C, while the experimental temperature is 39 °C. The error is just over 5%, but we must consider that not all the errors are attributable to the model, as the temperature of the external environment is not exactly known. In any case, numerical simulations provide an acceptable comparison with experimental results.

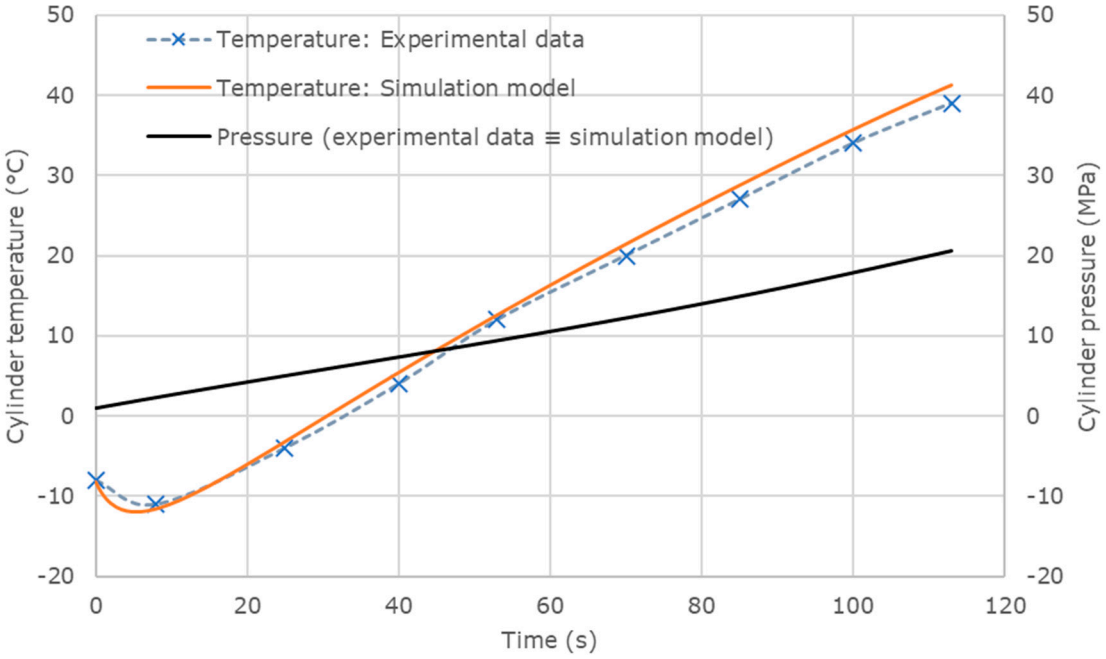

Figure 5. Comparison between experimental [20] and numerical results.

6. The Case Study and Simulation Results

6.1. The Case Study

The model has been applied to simulate the loading and the unloading processes of the CNG tanker that is being designed under the GASVESSEL project; see Table 2.

The on-board compression station consists of two double-stage centrifugal compressors that can work in parallel. The polytropic efficiency varies from 0.5 near the choke point up to the maximum value, which is supposed to be 0.73. The outlet temperature of both the intercooler and cooler is set to 40 °C.

Regulation is carried out by means of a throttling valve and variation of speed. The objective is to optimize the mass flow rate, keeping the absorbed power below the maximum design value of 10 MW.

The loading process is carried out from a storage terminal constituted of a Floating Production Storage and Offloading (FPSO) unit, whose water volume is supposed to be twice the ship water volume. The FPSO initial pressure is 240 bar. The initial pressure in the ship gas cylinders is 30 bar, and the loading process ends when it reaches the design value of 300 bar. The forced loading phase starts when the mass flow rate due to the free loading falls below 20 kg/s.

The unloading process is carried out in a pipeline at a constant pressure of 120 bar. The initial pressure in the ship gas cylinders is supposed to be the same reached at the end of the loading process, 300 bar, neglecting the possible variations due to the ship engines consumption and to the heat exchange with the surroundings. The unloading process ends when it reaches the final value of 30 bar. Such a final value has been imposed considering that the remaining gas must be sufficient to guarantee the fuel for the return journey. The forced unloading phase starts when the mass flow rate due to the free unloading falls below 20 kg/s. In these conditions, the pressure in the gas cylinders remains for a while higher than that in the pipeline: this requires acting on the lamination valve to make the suction pressure lower than 120 bar, so allowing the normal operating conditions of the compressors.

Two calculation hypotheses have been taken into account: i.e., adiabatic or not adiabatic pressure vessels. The first is useful as a term of comparison, while the second is more realistic. In the not adiabatic case, the environmental temperature is another variable of the model: the temperature of nitrogen filling the holds has been set to 40 °C and 5 °C in summer and winter conditions, respectively.

The results discussed below have been obtained considering, as a term of comparison for further analysis, the compression of pure methane.

6.2. Simulation Results: Adiabatic Processes

Calculations have been carried on by setting the terms relating to the heat exchange in the pressure vessels to zero (see Equations (6) and (7) of the tank model).

The results obtained with reference to the loading process are summarized in Figures 6–11. They show the trend as a function of time of pressure and temperature in the storage terminal (Figure 6) and in the pressure vessels (Figure 7), the mass flow rate (Figure 8), the mass of CNG in the pressure vessels (Figure 9), the compression ratio (Figure 10), and the compressor power (Figure 11), respectively.

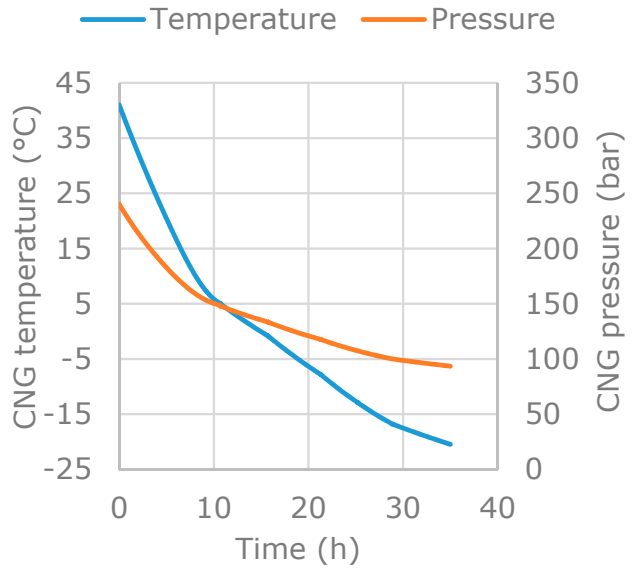

Figure 6. Storage terminal CNG conditions (adiabatic loading).

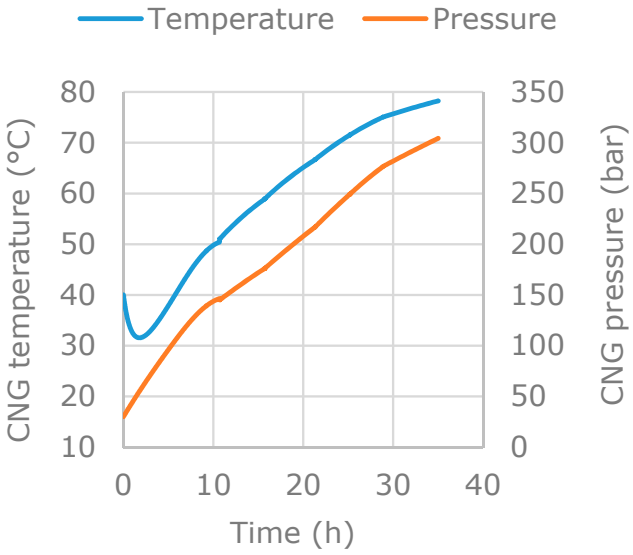

Figure 7. Pressure vessels CNG conditions (adiabatic loading).

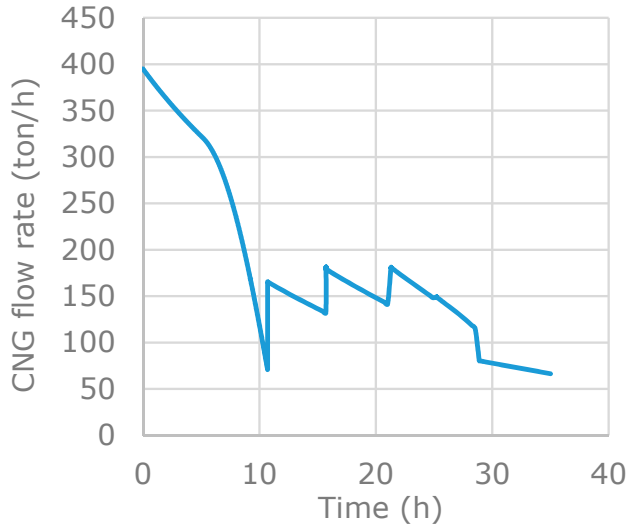

Figure 8. CNG flow rate (adiabatic loading).

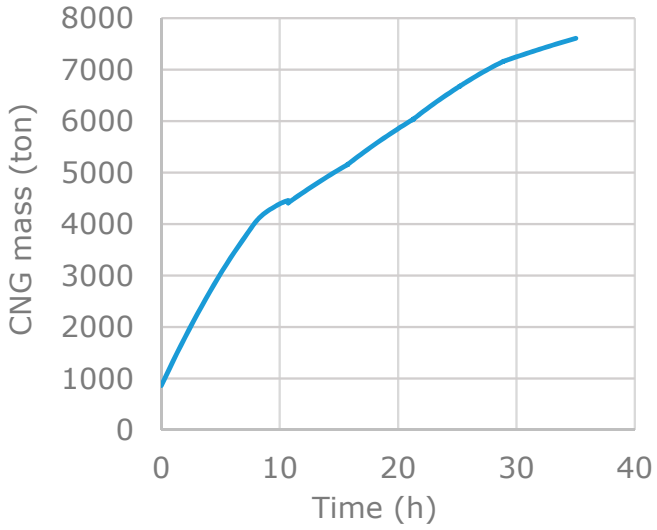

Figure 9. Mass of CNG in the pressure vessels (adiabatic loading).

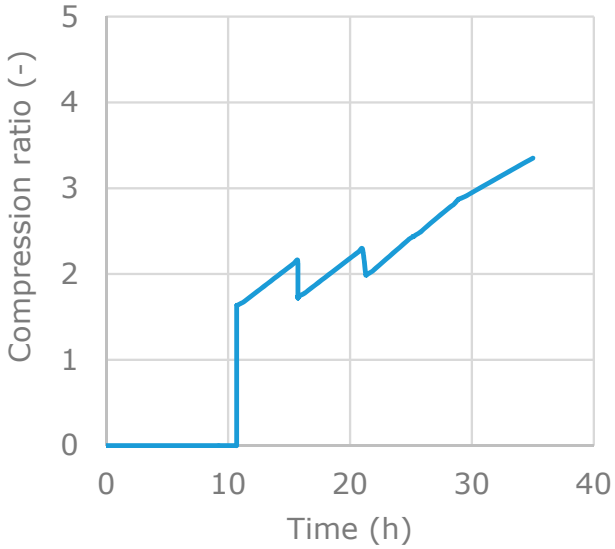

Figure 10. Compression ratio (adiabatic loading).

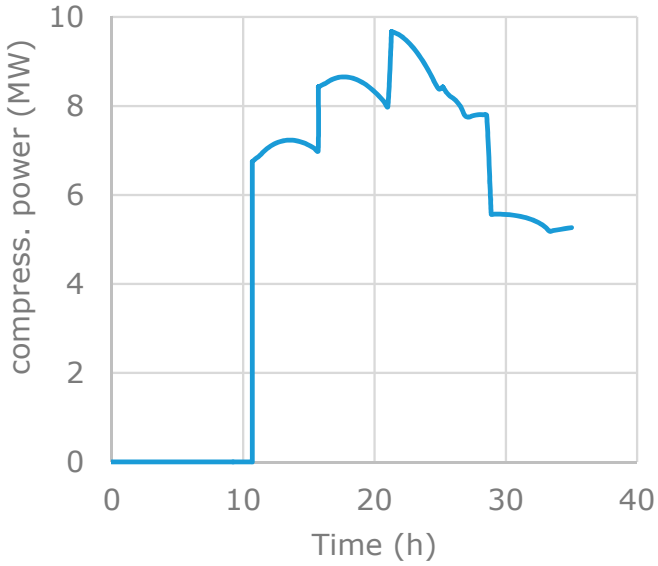

Figure 11. Compressor power (adiabatic loading).

The entire loading phase needs about 35 h. The singular point that can be observed at time 11 h in the flow rate, compression ratio, and compressor power curves corresponds to the passage from the free loading to the forced loading phase with the start of the two compressors. Therefore, the forced loading phase takes 24 h. The singularities visible during this phase, between 11 h and 25 h, are due to the regulation of the compressor with variation of the rotational speed, starting at 10,000 rpm up to 11,500 rpm, to maintain the flow rate within the range between the pumping and flooding limits. The last singularity, at about 28 h, corresponds to the switching-off of one of the two compressors, due to the reduction of mass flow rate that occurs toward the end of the process.

The loaded mass is about 6750 ton. The overall mean flow rate is about 192 ton/h but, when compressors are running, the mean value is 133 ton/h. The maximum compression ratio is 3.3, obviously at the end of the forced loading phase. The fuel consumption is 36 ton (≃0.5% of the total cargo), and the specific energy consumption is 96 kJ/kg.

Particular attention requires, for the reasons discussed in paragraph 1, the temperature trend in the pressure vessels. Starting from the initial chosen value of 40 °C, at first, the temperature decreases by about 10 °C. As described in [7], it is due to the Joule–Thompson cooling effect that undergoes the gas in an isenthalpic expansion through an orifice. When it enters in a nearly empty cylinder, this cold gas mixes with and compresses the gas originally in the tank. The result is that the combined mixed gas temperature initially reduces. When the compression and conversion of supply enthalpy energy to cylinder internal energy overcomes the Joule–Thompson cooling effect, which becomes smaller as the cylinder pressure increases, the mixed gas temperature in the cylinder begins to increase [13]. It reaches 78 °C at the end of the process in the considered case, with an increment of 38 °C. This result is consistent with those found in [6], and it corresponds to a fill efficiency of 85%, in comparison with an ideal loading at the initial temperature of 40 °C.

The results obtained with reference to the adiabatic unloading process are summarized in Figures 12–16. They show the trend as a function of time of pressure and temperature in the pressure vessels (Figure 12), the mass flow rate (Figure 13), the mass of CNG in the pressure vessels (Figure 14), the compression ratio (Figure 15), and the compressor power (Figure 16), respectively.

The entire unloading process needs about 46 h, divided into 12 h for the initial free phase and 34 h for the subsequent forced phase, as clearly shown by the compressor power diagram. The 10 h more than the loading phase are due to the compressor working at higher compression ratio values. As in the previous case, the singularities in the flow rate, compression ratio, and compressor power curves during the forced phase are due to the speed regulation of the compressor.

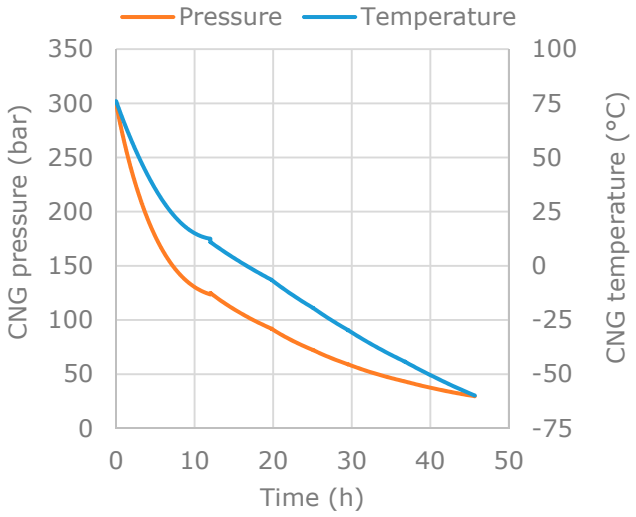

Figure 12. Pressure vessels CNG conditions (adiabatic unloading).

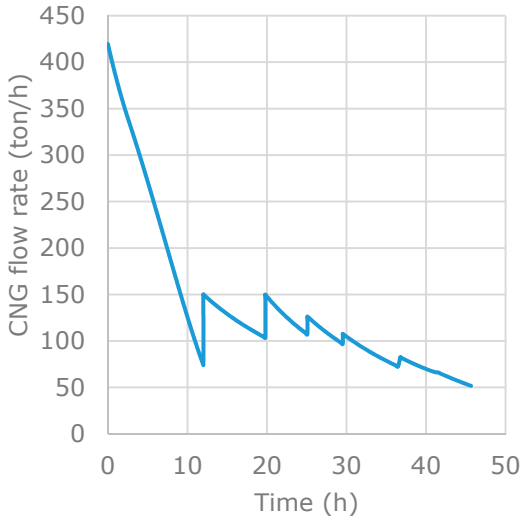

Figure 13. CNG flow rate (adiabatic unloading).

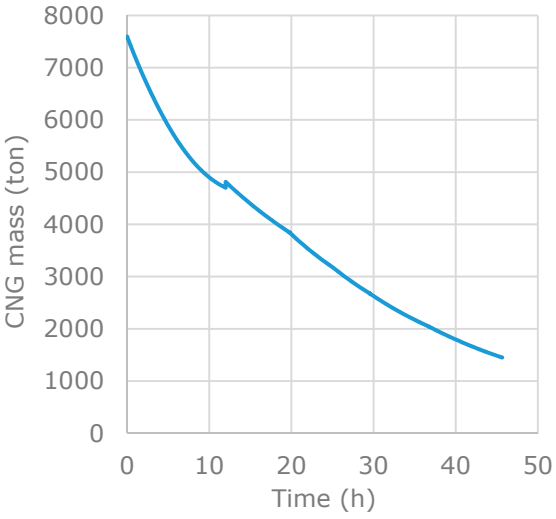

Figure 14. Mass of CNG in the pressure vessels (adiabatic unloading).

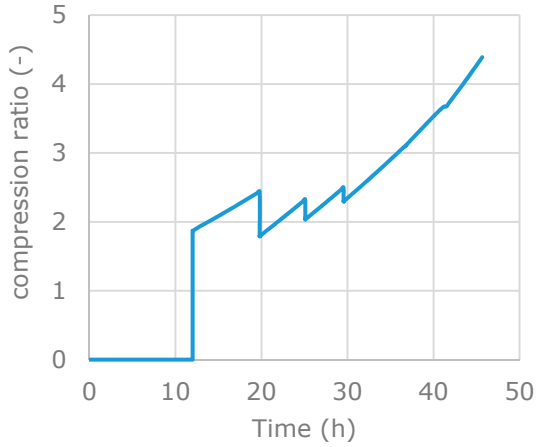

Figure 15. Compression ratio (adiabatic unloading).

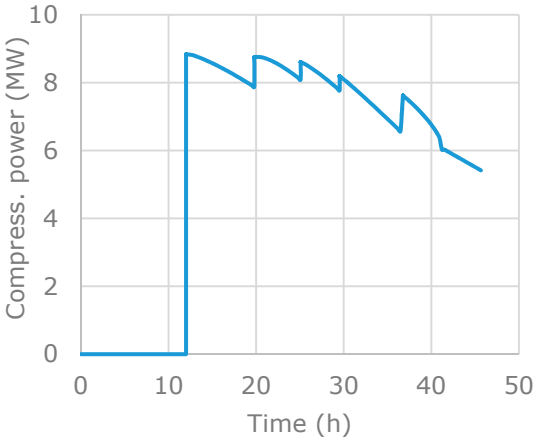

Figure 16. Compressor power (adiabatic unloading).

The unloaded mass is about 6150 ton. The residual mass left in the cylinders is 600 ton higher than that at the start of the loading process, at the same pressure of 30 bar: this is due to the very low temperature, about 60 °C below zero, reached at the unloading end. In fact, such a low temperature cannot be tolerated because it could lead to the condensation of propane and butane, compromising the normal functionality of the compressor. To avoid this, the heater (Figure 1) must be able to guarantee a gas temperature of at least 4 °C.

The mean flow rate is about 135 ton/h. The fuel consumption is equal to 51 ton (≃0.7% of the total cargo), and the specific energy consumption is 151 kJ/kg.

Taking into account both the loading and unloading processes, the adiabatic overall fuel consumption is ≃1.14% of the total cargo, corresponding to about three pressure vessels.

6.3. Simulation Results: Not Adiabatic Processes

The heat exchange between the pressure vessels and the nitrogen of the holds has been calculated at each time step. The overall heat transfer coefficient has been obtained calculating the internal and external convective heat exchange coefficients according to Section 4.1, while the heat conduction through the composite wall of the GASVESSEL cylinders has been obtained on the basis of the specifications given in Table 3.

From the temperature trends in the pressure vessels obtained in the previous case of adiabatic loading and unloading, it can be deduced that the heat exchange with the environment should allow improving both the filling of the cylinder during the loading phase and the emptying during the unloading phase. In fact, the heat exchange with the environment contrasts both the heating of the accumulated gas in the first case and the cooling of the residual one in the second. However, it is

evident that the improvement will be less significant in the loading phase during the summer and in the unloading phase during the winter. The results obtained with the simulations under these two conditions, which can be considered of greater operational interest, are presented below.

Table 3. GASVESSEL project: CNG vessel wall properties [4].

	Thickness (m)	Density (kg/m^3)	Specific Heat (J/kg/K)	Thermal Conductivity (W/m/K)
liner	0.005	7800	500	60
carbon fiber epoxy	0.035	938	1494	1

In the case of summer loading, the loaded mass was 7290 ton, with an increment of 8% with respect to the adiabatic case. However, the duration of the process is extended by 45%, from 35 h to about 51 h. The increment of 16 h is almost entirely due to the greater mass loaded during the forced phase (39 h instead of 24 h) at high compression ratios.

Figure 17 shows the trend as a function of time of pressure and temperature in the pressure vessels. By comparing the temperature trend with those of Figure 7, it can be observed that the initial cooling of the CNG in the vessels disappears, that the maximum temperature is 70 °C instead of 78 °C, and that it occurs at about half the duration of the process. Most importantly, the final temperature reduces to 60 °C, giving the cited increment of the loaded mass. The compressor power trend reported in Figure 18 is quite similar to that of the adiabatic case of Figure 17 until time 35 h; then, the reduction of temperature leads to a final rise of the power, following the rise of the rotational speed and compression ratio. The maximum value of the last one increases with respect to the adiabatic case from 3.3 to 4.3.

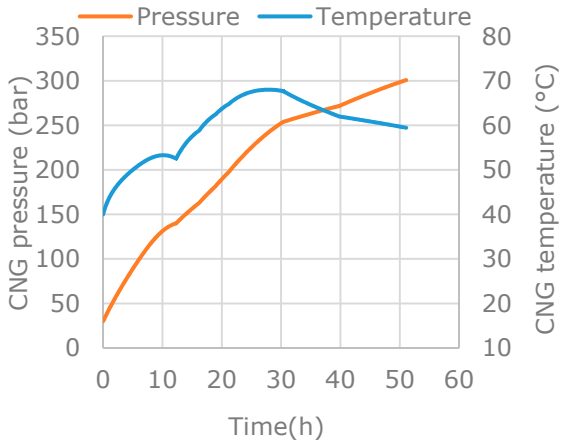

Figure 17. Pressure vessels CNG conditions (summer loading).

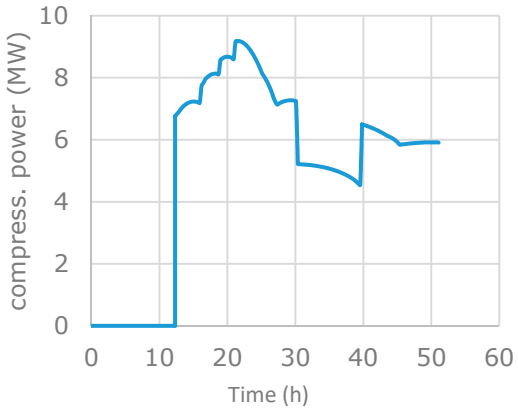

Figure 18. Compressor power (summer loading).

As a whole, the mean flow rate decreases from 192 to 143 ton/h, the fuel consumption increases from 36 to 51 ton (≃ 0.6% of the total cargo), and the specific energy consumption reaches 134 kJ/kg, instead of 96 kJ/kg.

As far as the heat exchange is concerned, the peak power dispersed by the single cylinder is equal to 32 kW, and the energy dispersed in the hold is 658 kWh. Considering that there are 256 cylinders in the hold, which are filled at the same time, there is a total maximum dispersed power of 8.2 MW and a total dispersed energy of 168.448 kWh.

In the case of winter unloading, the unloaded mass is 7025 ton, with an increment of about 14% in comparison with the adiabatic case. The residual mass is reduced of 265 ton with respect to the adiabatic calculation, due to the higher final temperature. Figure 19 shows the trend as a function of time of pressure and temperature in the pressure vessels: the minimum temperature is −25 °C, which is reached at about two-thirds of the unloading time, while the final temperature is −17 °C (remember that in the adiabatic case, the minimum was −60 °C at the end of the process). The unloading process lasts 55 h, 44 of which are due to the forced phase. The increments with respect to the adiabatic case are of 9 and 10 h, respectively. The mean flow rate is about 119 ton/h against 135 ton/h. The fuel consumption goes from 51 ton to 67 ton (≃1% of the total cargo), and the specific energy consumption goes from 151 kJ/kg to 183 kJ/kg. The compressor adsorbed power, reported in Figure 20, shows a trend very similar to those of the adiabatic case of Figure 16.

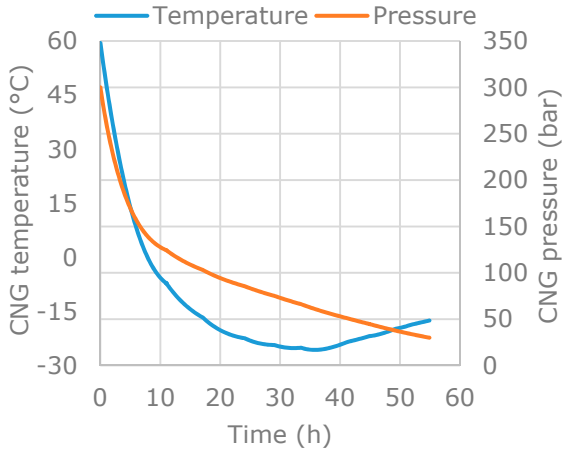

Figure 19. Pressure vessels CNG conditions (winter unloading).

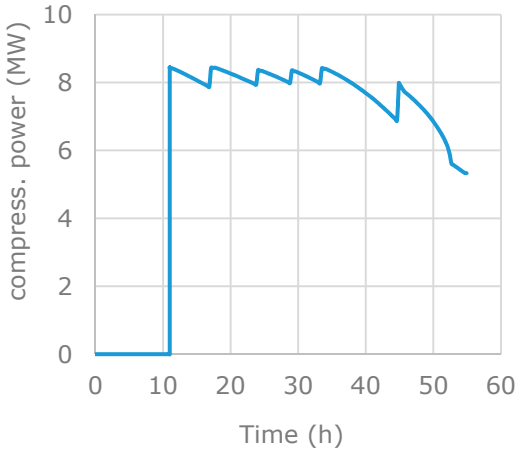

Figure 20. Compressor power (winter unloading).

Considering the overall balances of the non-adiabatic process, the total fuel consumption is ≃1.45% of the total cargo, corresponding to about 3.5 pressure vessels.

7. Future Application: The Hydrogen Case

The use of hydrogen as an energy carrier is a very topical issue, because it allows meeting, together with the use of fuel cells, the requirements of zero local emissions. One aspect that limits the diffusion on a large scale of hydrogen is its low volumetric energy density. Pure hydrogen reaches acceptable storage densities only at cryogenic temperatures, at −253 °C, at high pressure, or both at high pressure and low temperature. The solution with the higher level of technology maturity is the storage at high pressure, at the same pressure levels considered for LNG.

In considering the loading and unloading processes of hydrogen, it must also be taken into account that the energy density of H_2 is much less dependent on temperature than that of methane, as shown in Figure 21. Moreover, the compressor efficiency changes with molecular weight, in particular with the volumetric ones. It is mainly due to the valve loss power, which is lower with low molecular weight. For example, as reported in [21], the maximum adiabatic efficiency drops from 93% with CH_4 to a still very good 88% with H_2 at a compression ratio of 3 but from 91% to 70% at a compression ratio of 1.4.

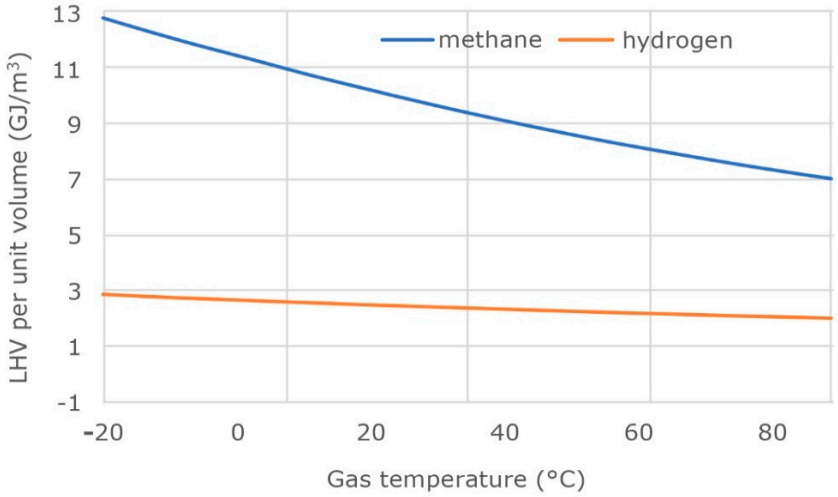

Figure 21. Energy density of CH_4 vs. H_2.

Simulations carried out with H_2 on the same plant considered for the loading and unloading of CNG show that the temperature reached at the end of the loading is much higher, as can be seen comparing Figure 7 with Figure 22, with reference to the adiabatic case. In addition, the maximum required compressor power becomes higher and exceeds the maximum design value of 10 MW, as shown in Figure 23.

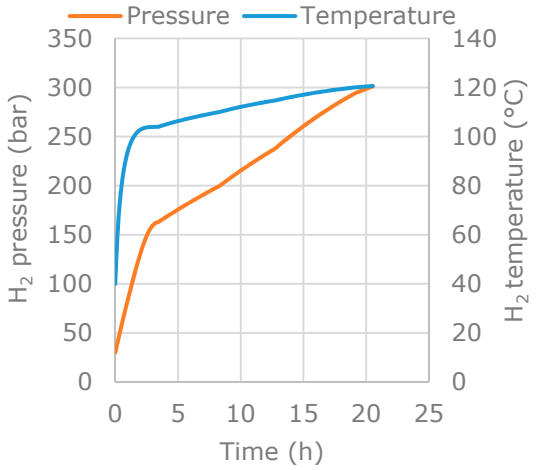

Figure 22. Pressure vessels conditions (H_2 loading).

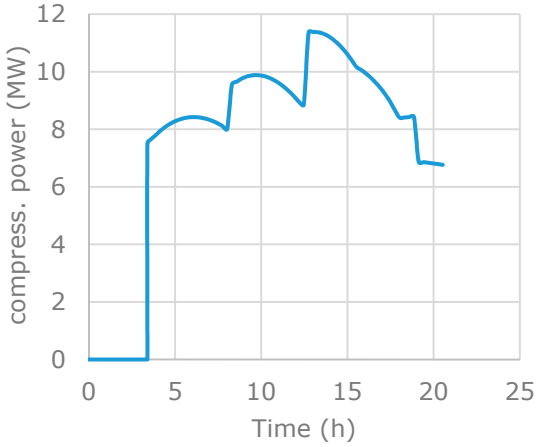

Figure 23. Compressor power (H_2 loading).

Taking into account the entire process, the specific energy consumption is almost ten times higher than that of methane, as reported in Table 4.

Table 4. Loading process: methane vs. hydrogen.

	Methane	**Hydrogen**
loading time [h]	35	21
final pressure [bar]	300	300
loaded mass [ton]	7609	724
loaded volume [Nm^3]	10,601,922	8,157,685
stored energy @20 °C [MWh]	130,278	31,136
compressors energy [kWh]	180,575	163,636
fuel consumption [%]	0.5	1.7
specific energy consumption [kJ/kg]	96	945
num. of pressure vessels used	1	3.5

8. Conclusions

CNG technology can be advantageous over LNG for transporting by ship small quantities of gas over short distances, up to 3000–5000 km. However, these advantages are connected to the development of advanced technologies for the design and construction of lightweight and safe pressure vessels for CNG carriers. The vessels loading and unloading processes also must be optimized from the points of view of timing and energy consumption, because they have an impact on the economic feasibility of the whole CNG transport project.

The simulation model developed for this purpose proved to be a useful tool for the study of the loading and unloading system. The application of the model to a CNG carrier with the specifications of the GASVESSEL project made it possible to highlight the following points, depending on the calculation hypotheses on the heat exchange of the tanks with the hold:

- The time required for the loading process varies between 35 and 51 h, and for the unloading process, it varies between 46 and 55 h;
- The temperature in the pressure vessels varies at the end of the loading process between 78 and 60 °C, while at the end of the unloading process, it varies between −60 and −17 °C. In the first case, the relatively high temperature reduces the fill efficiency of the vessels, while in the second case, the low temperature is worrying for the proper functioning of the compressor, so that a gas heater is required;
- The energy consumption can vary in the range of 150–180 kJ for a unit mass of CNG;
- The total fuel consumption of the processes varies between 1.14% and 1.45% of the total cargo.

The next research goals are performing some experimental tests on the tanks that will allow the model to be fine-tuned. In the future the model will be integrated in a ship overall energy simulation model. As regards the aspects related to safety, the rules and regulatory requirements will be applied currently being issued by the certification bodies, such as those by the American Bureau of Shipping [22].

Author Contributions: R.T. conceived the presented idea and was responsible of the research. R.T. and D.M. designed the model, and G.M. designed the computational framework and performed the data presentation. All authors have read and agreed to the published version of the manuscript.

Funding: The project has received funding from the European Union's Horizon 2020 research and innovation programme under grant agreement No 723030.

Conflicts of Interest: The authors declare no conflict of interest.

Nomenclature

Acronyms

CAPEX	CAPital EXpenditure
CNG	Compressed Natural Gas
FPSO	Floating Production Storage and Offloading
LNG	Liquefied Natural Gas
NG	Natural Gas
OPEX	Operating EXpenditure

Symbols

A	flow area [m^2]
C_1	C_g/C_v [-]
C_d	outflow coefficient [-]
C_g	gas flow sizing coefficient [$lb/h/(psia \cdot lb/ft^3)^{0.5}$]
C_p	constant pressure specific heat [J/kg/K]
C_v	fluid flow sizing coefficient [$lb/h/(psia \cdot lb/ft^3)^{0.5}$]
D	diameter [m]
h	enthalpy [J/kg]
k	specific heat ratio [-]
L	length [m]
m	mass [kg]
$\dot{m}$	mass flow rate [kg/s]
n	polytropic exponent [-]
p	pressure [Pa]
P	power [W]
Q	heat [J]
R	gas constant [J/kg/K]
S	surface [m^2]
T	temperature [K]
u	internal energy [J/kg]
v	velocity [m/s]
Z	compressibility factor [-]
α	convective heat exchange coefficient [$W/m^2/K$]
β	compression ratio [-]
ϱ	density [kg/m^3]
η	efficiency [-]
λ	Darcy friction factor [-]

Subscripts

O1	stagnation condition at compressor inlet
amb	ambient

hex	heat exchanger
r	receiving vessel
i	inlet, internal
o	outlet
e	external
p	polytropic
w	cylinder wall

References

1. ExxonMobil. *Outlook for Energy: A Perspective to 2040*; ExxonMobil Corporation: Irving, TX, USA, 2019.
2. Poli, R.; Scaroni, P. *Tranpsorting Natural Gas by Sea, Encyclopaedia of Hydrocarbons*; Istituto della Enciclopedia Italiana G. Treccani: Roma, Italy, 2005.
3. Tractebel Engineering, S.A. *CNG for Commercialization of Small Volumes of Associated Gas*; World Bank: Washington, DC, USA, 2015.
4. GASVESSEL-Compressed Natural Gas Transport System. Available online: www.gasvessel.eu (accessed on 30 August 2020).
5. Kuczynski, S.; Liszka, K.; Laciak, M.; Olijnyk, A.; Szurlej, A. Experimental Investigations and Operational Performane Analysis on Compressed Natural Gas Home Refueling System (CNG-HRS). *Energies* **2019**, *12*, 4511. [CrossRef]
6. Kountz, K.J. Modeling the fast fill process in natural gas vehicle storage cylinders. In Proceedings of the Spring National Meeting of the ACS, San Diego, CA, USA, 13–18 March 1994; pp. 462–469.
7. Farzaneh-Gord, M.; Deymi-Dashtebayaz, M.; Rahbari, H.R. Studying effects of storage types on performamce of CNG filling stations. *J. Nat. Gas Sci. Eng.* **2011**, *3*, 334–340. [CrossRef]
8. Khamforoush, M.; Moosavi, R.; Hatami, T. Compressed natural gas behaviour in a natural gas vehicle fuel tank during fast filling process: Mathematical modeling, thermodynamic analysis, and optimization. *J. Nat. Gas Sci. Eng.* **2014**, *20*, 121–131. [CrossRef]
9. Farzaneh-Gord, M.; Reza-Rahbari, H.; Deymi-Dashtebayaz, M. Effects of Natural Gas Compositions on CNG Fast Filling Process for Buffer Storage System. *Oil Gas Sci. Technol.* **2014**, *69*, 319–330. [CrossRef]
10. Farzaneh-Gord, M.; Niazmand, A.; Deymi-Dashtebayaz, M. Effects of natural gas composition on CNG (compressed natural gas) reciprocating compressors performance. *Energy* **2015**, *90*, 1152–1162. [CrossRef]
11. Zhang, G.; Brinkerhoff, J.; Li, R.; Forsberg, C.; Sloan, T. Analytical and numerical study on the fast refill of compressed natural gas with active heat removal. *J. Nat. Gas Sci. Eng.* **2017**, *45*, 552–564. [CrossRef]
12. Cen, K.; Song, B.; Jia, W.; Li, W.; Han, T. Numerical modeling of the dynamic filling process of high-pressure tankers for marginal gas wells. *J. Nat. Gas Sci. Eng.* **2019**, *72*, 103029. [CrossRef]
13. Farzaneh-Gord, M. Real and ideal gas thermodynamic analysis of single reservoir filling process of natural gas vehicle cylinders. *J. Theor. Appl. Mech.* **2011**, *41*, 21–36.
14. Mokhatab, S.; Poe, W.A.; Mak, J. *Handbook of Natural Gas Transmission and Processing*; Elsevier: Amsterdam, The Netherlands, 2015.
15. Setzmann, U.; Wagner, W. A New Equation of State and Tables of Thermodynamic Properties for Methane Covering the Range form the Melting Line to 625 K at Pressure up to 1000 MPa. 6. *J. Phys. Chem. Ref. Data* **1991**, *20*, 1061–1151. [CrossRef]
16. Kunz, O.; Wagner, W. The GERG-2008 Wide-Range Equation of State for Natural Gases and Other Mixtures: An Expansion og GERG-2004. *J. Chem. Eng. Data* **2012**, *57*, 3032–3091. [CrossRef]
17. Woodfield, P.L.; Monde, M.; Takano, T. Heat transfer Characteristics for Practical Hydrogen Pressure Vessels Being Filled at High Pressure. *J. Therm. Sci. Technol.* **2008**, *3*, 241–253. [CrossRef]
18. Aspen Tech Inc. *Aspen HYSYS v8.8 Unit Operation Guide*; Aspen Tech Inc.: Bedford, MA, USA, 2019.
19. Kirmaen, J.; Niemela, I.; Pyotsia, J.; Simula, M.; Hauhia, M.; Riihilathi, J.; Lempinen, V.; Koukkuluoma, J.; Kanerva, P. *Flow Control Manual*; Metso Automation Inc.: Helsinki, Finland, 2011.
20. Kim, C.J.; Cho, S.M.; Kim, E.J.; Yoon, K.B. The study on the internal temperature change of type 3 and type 4 composite cylinder during filling. In Proceedings of the 5th International Conference on Hydrogen Safety (ICHS 2013), Brussels, Belgium, 9–11 September 2013.

21. Phillippi, G. Basic thermodynamics of reciprocating compression. In Proceedings of the 45th Turbomachinery & 32nd Pump Symposia, Houston, TX, USA, 12–15 September 2016.
22. American Bureau of Shipping. *Guide for Vessels Intended to Carry Compressed Natural Gases in Bulk*; American Bureau of Shipping: Houston, TX, USA, 2020.